JSLHR

Research Article

Influence of Embedded Fibers and an Epithelium Layer on the Glottal Closure Pattern in a Physical Vocal Fold Model

Yue Xuan[a] and Zhaoyan Zhang[a]

Purpose: The purpose of this study was to explore the possible structural and material property features that may facilitate complete glottal closure in an otherwise isotropic physical vocal fold model.
Method: Seven vocal fold models with different structural features were used in this study. An isotropic model was used as the baseline model, and other models were modified from the baseline model by either embedding fibers aligned along the anterior–posterior direction in the body or cover layer, adding a stiffer outer layer simulating the epithelium layer, or a combination of the 2 features. Phonation tests were performed with both aerodynamic and acoustic measurements and high-speed imaging of vocal fold vibration.
Results: Compared with the isotropic one-layer model, the presence of a stiffer epithelium layer led to complete glottal closure along the anterior–posterior direction and strong excitation of high-order harmonics in the resulting acoustic spectra. Similar improvements were observed with fibers embedded in the cover layer, but to a lesser degree. The presence of fibers in the body layer did not yield noticeable improvements in glottal closure or harmonic excitation.
Conclusion: This study shows that the presence of collagen and elastin fibers and the epithelium layer may play a critical role in achieving complete glottal closure.

Key Words: glottal closure, voice production, voice quality

An important feature of normal phonation is that the glottis remains closed for a considerable portion of one oscillation cycle. The glottal closure pattern (i.e., the speed and duration of glottal closure) is essential to the production of voice with harmonics at frequencies well above the oscillation frequency of the vocal folds (Stevens, 1998). In humans, it is often assumed that approximation of the vocal folds through arytenoid adduction is sufficient to achieve complete glottal closure in phonation. However, recent experiments using self-oscillating silicone-based physical models (Zhang, 2011; Zhang, Neubauer, & Berry, 2006b, 2009; readers are referred to Kniesburges et al., 2011, for a comprehensive review of the use of physical vocal fold models in voice research) showed that isotropic (i.e., the material properties are the same along different directions) physical models often vibrated with incomplete glottal closure at onset despite the two vocal fold models being brought into contact at rest. During vibration, although the isotropic vocal fold models were able to move back toward glottal midline, the contact between the two vocal folds, if it happened at all, was brief and often occurred only at the middle portion along the anterior–posterior (AP) direction. Because of this incomplete glottal closure, the produced sound was breathy in quality. This contrasts with human vocal folds, which are able to vibrate with the glottis closed for a considerably long portion of the oscillation cycle at a large range of laryngeal conditions (van den Berg & Tan, 1959). In addition, the isotropic physical models often exhibited out-of-phase motion along the AP direction, particularly at the end of the closing phase of the oscillation cycle (Mendelsohn & Zhang, 2011; Zhang, 2011). In contrast, human vocal folds, at least the membranous portion, often move in-phase along the AP direction during normal phonation.

Our previous efforts to overcome these deficiencies of the isotropic physical model focused on reducing the static vertical and lateral deformation of the physical vocal fold model when subjected to the subglottal pressure. The underlying rationale was that reducing the mean glottal opening would shift the equilibrium position of vocal fold vibration toward the glottal midline and thus facilitate complete glottal closure. As a first attempt along this direction, Zhang et al. (2006a) used a vertical restraint applied to the lateral half of the superior surface of the vocal fold model, which significantly suppressed the vertical motion of the vocal fold model and facilitated complete glottal closure. As there is

[a]University of California, Los Angeles School of Medicine
Correspondence to Zhaoyan Zhang: zyzhang@ucla.edu

Editor: Rhea Paul
Associate Editor: Scott Thomson
Received March 20, 2013
Revision received May 28, 2013
Accepted August 12, 2013
DOI: 10.1044/2013_JSLHR-S-13-0068

Disclosure: *The authors have declared that no competing interests existed at the time of publication.*

no obvious counterpart of this vertical restraint in human physiology, it was hypothesized that this restraining effect can be achieved through either stiffening the body layer, which presumably can be achieved by the contraction of the thyroarytenoid muscle, or increasing vocal fold stiffness along the AP direction, which can be achieved through the action of the cricothyroid muscle. This hypothesis was further explored in Zhang (2011), which showed that both mechanisms led to reduced mean glottal opening and increased production of high-order harmonic energy in the resulting sound spectra. Despite these improvements, glottal closure in these models was often brief, with an almost-zero closed quotient (the fraction of the cycle that the glottis remains closed). Stiffening the body layer in an isotropic physical model also led to strong excitation of AP out-of-phase motion. More importantly, activation of these restraining mechanisms in humans requires strong contraction of laryngeal muscles, and thus is not effective in low-pitch, low-intensity phonation conditions.

Thus, it seems that, in addition to laryngeal muscle activation, the human vocal folds have some inherent structural or material features that facilitate complete glottal closure during human phonation. Identifying these features of the vocal folds has the potential to significantly improve clinical management of voice disorders and would also allow us to design physical models that are capable of producing more realistic vibration patterns. Some clues regarding what these structural features might be can be found in previous studies. Zhang (2011) showed that vocal folds with a higher stiffness in the AP direction due to vocal fold elongation improved glottal closure. A large AP-to-transverse stiffness ratio also suppressed the AP out-of-phase motion and thus led to a more in-phase medial–lateral motion along the AP direction during phonation (Zhang, 2011). Thus, it is possible that a naturally anisotropic vocal fold model is able to produce a relatively stronger medial–lateral motion and thereby achieve complete glottal closure. Indeed, early studies by Hirano and Kakita (1985) showed that due to the presence of muscle fibers in the muscle layer and collagen and elastin in the lamina propria, the vocal folds are at least transversely isotropic. On the other hand, recent studies showed that a water-filled latex tube model of the vocal folds (Ruty, Pelorson, Van Hirtum, Lopez-Arteaga, & Hirschberg, 2007) was able to achieve complete glottal closure and a considerably large closed quotient (Krebs, Artana, & Sciamarella, 2010). In humans, the epithelium is a very thin layer (~50–80 μm thickness) with a Young's modulus (~100 kPa) that is much larger than the inner layers (Hirano & Kakita, 1985). Gunter (2003) showed that, for a given subglottal pressure, the maximum glottal opening decreased with increasing stiffness of the outer epithelium layer. Murray and Thomson (2012) showed that the combination of a stiff epithelium layer and an extremely soft cover layer led to an alternating convergent–divergent motion of the vocal fold motion. These studies suggest that the presence of the epithelium layer may also facilitate complete glottal closure.

Physical models with features approximating the collagen and elastin fibers and the epithelium layer have been developed in previous studies. For example, Shaw, Thomson, Dromey, and Smith (2012) embedded acrylic and polyester fibers in the surface layer of an otherwise linear two-layer silicone physical model to achieve vocal fold material nonlinearity. Titze and colleagues (Chan, Titze, & Titze, 1997; Titze, Schmidt, & Titze, 1995) attached a silicone epithelium membrane to a stainless steel flat surface and filled the air gap with fluids of varying viscosities to study the dependence of phonation threshold pressure on vocal fold viscosity and geometry. The latex membrane in the water-filled latex tube vocal fold model in Ruty et al. (2007) functioned equivalently as an epithelium layer. Recently, the effects of an epithelium layer and a ligament layer with fibers embedded along the AP direction on vocal fold vibration (e.g., medial surface profile and the vertical phase difference) were investigated in a multilayer silicone vocal fold model (Murray & Thomson, 2012). However, these previous studies generally focused on other aspects of phonation, and the possible effects of the presence of embedded fibers and a stiffer epithelium layer on the glottal closure pattern and sound production have not been investigated.

The goal of this study was to investigate the possible influence of the epithelium and embedded fibers on the glottal closure pattern and sound production in an otherwise isotropic one-layer physical model. The use of a one-layer baseline model instead of a multilayer baseline model as in previous studies (Murray & Thomson, 2012; Zhang, 2011) was to approximate the conditions of minimum laryngeal contraction and thus focus this study on the effects of features inherent to the vocal folds (i.e., collagen and elastin fibers and the epithelium layer) rather than those induced by laryngeal muscle activation. We will show that adding a thin stiffer outer layer to an otherwise homogenous model led to complete glottal closure and strong excitation of high-order harmonics. Similar improvement in the glottal closure pattern was also achieved with fibers embedded in the cover layer.

Method

The details of the experimental setup for phonation tests have been described in previous studies (Zhang, 2011; Zhang et al., 2006a, 2006b). As shown in Figure 1, the setup consisted of an expansion chamber (with a rectangular cross-section of 23.5×25.4 cm^2 and a length of 50.8 cm) simulating the lungs, an 11-cm-long straight circular PVC tube (inner diameter of 2.54 cm) simulating the tracheal tube, and a self-oscillating vocal fold model. The expansion chamber was connected upstream to a pressurized airflow supply through a 15.2-m-long rubber hose. To focus on the effects of vocal fold structural features on the glottal closure pattern and avoid possible source-tract interaction, no vocal tract was used in this study.

Seven vocal fold models of identical geometry but different structural compositions were fabricated and used in this study. All vocal folds had a medial surface thickness of 2 mm, a lateral surface thickness of 9 mm along the inferior–superior direction, and a depth of 7.5 mm along the medial–lateral direction, as shown in Figure 2a. A one-layer isotropic

Figure 1. Schematic of the experimental setup.

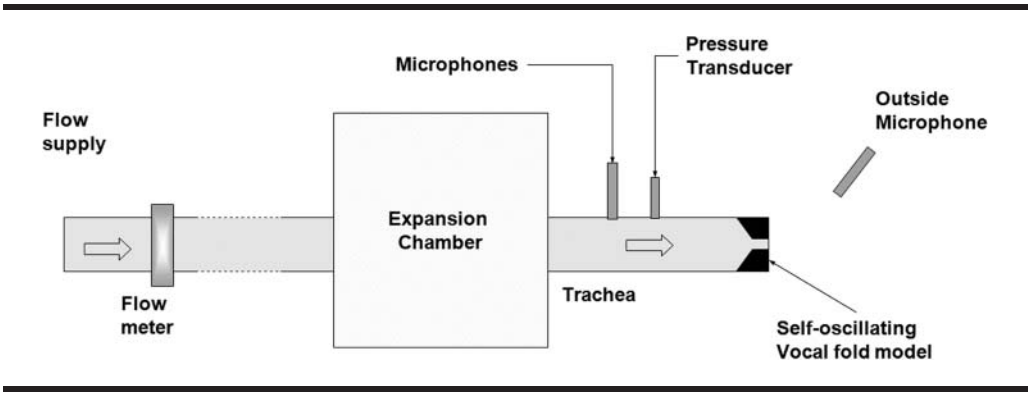

model as used in previous studies (Thomson, Mongeau, & Frankel, 2005; Zhang, 2011; Zhang et al., 2006a, 2006b) was used as the baseline model (M1), whereas models M2–M6 included a stiffer thin epithelium layer, embedded fiber bundles, or both features (Table 1). The first six models (M1–M6) had a length of 17 mm along the AP direction. M7 was identical to M1 except for a reduced length of 12 mm. All models (M1–M7) were fabricated by mixing a two-component silicone compound solution (Ecoflex 0030, Smooth-on, Easton, PA) with a silicone thinner (Smooth-on, Easton, PA) at a 1:1:5 weight ratio. M1–M6 were made at the same time using the same mixture; M7 was made at a different time but with an identical mixture ratio. The Young's modulus of the fully cured mixture was measured to be approximately 2.5 kPa using an indentation method (Chhetri, Zhang, & Neubauer, 2011). Our previous experience showed that models of the same composition ratios but fabricated at different times were quite consistent in terms of the measured Young's modulus, which varied often less than 10%. The epithelium layer was added by evenly spreading three drops of a silicone mixture solution (Ecoflex 0030, weight ratio of 1:1, with a Young's modulus of 60 kPa) over the surface of a baseline model. The thickness of the epithelium layers was about 130±20 μm, as measured after phonation tests using a digital microscope (Olympus DP70, Center Valley, PA) with 100x magnification. For each model with embedded fibers, a total of seven ultra gel-spun polyethylene fiber bundles (Ultra GSP thread, 50 denier, WAPSI, Inc. Mountain Home, Arkansas), each 4-mm long, were aligned along the AP direction at desired locations within the vocal fold model, as shown in Figures 2b and 2c. Each fiber bundle had a diameter of 60 μm and a Young's modulus in the order of 60 GPa, as estimated from tensile tests. For models with fibers in the cover layer, the fiber bundles were first aligned in the mold before the silicone mixture solution was poured into the mold. For models with fibers in the body layer, the silicone compound solution was first poured to fill the bottom half of the mold and then the fiber bundles were added to the top of the half vocal fold model before the silicone compound solution was fully cured. Additional silicone compound solution (the same mixture solution as the bottom half) was then added to fill the top half of the mold. No pretension was applied to the fiber bundles, and the bundles were not fixed to the anterior or posterior ends. Before alignment, the fiber bundles were soaked in a silicone primer (PR-1200 RTV, Dow Corning, Midland, MI) and then dried for 30 min in order to enhance bonding between the silicone rubber and the fiber bundles so that the fibers would not detach from the silicone rubber matrix during vibration. All models were cured at 75 °C for 1 hr after degassing and then at room temperature for 2 days. As in previous studies, the fully cured vocal fold models were then glued to a rectangular groove on the medial surface of two acrylic plates. The surface of the vocal fold model was further sprayed with a release agent (Ease Release 200, Smooth-on, Easton, PA) to prevent the two vocal folds from sticking to each other during vibration.

For each vocal fold model, the subglottal pressure was gradually increased in discrete increments from zero to approximately 20% above the phonation threshold pressure. At each step, with a delay of approximately 1–2 s after the flow rate change, the mean subglottal pressure (measured at 2 cm from the entrance of the glottis using a Baratron 220D pressure transducer), mean flow rate (MKS 558A mass-flow meter), subglottal acoustic pressure inside the tracheal tube (2 cm from the entrance of the glottis using a B&K 4182 probe microphone), and outside acoustic pressure (approximately 20 cm downstream and approximately 30° off axis using a B&K 2669 microphone) were recorded for a 1-s period at a sampling rate of 50 kHz. The phonation threshold pressure, onset flow rate, and onset frequency were then extracted as the mean subglottal pressure, mean flow rate, and fundamental frequency at onset, as described in Zhang et al. (2006b). A high-speed camera (Fastcam-Ultima APX, Photron Unlimited, Inc.) was used to record vocal fold vibration from a superior view at 2000 fps from which the glottal area waveform was extracted using a MATLAB-based program.

Results

Figure 3 shows the phonation threshold pressure and flow rate, the onset frequency, and the outside acoustic pressure at onset for all seven vocal fold models. Adding a stiffer outer layer led to a significant increase in all four

Figure 2. Sketch of the coronal cross-sectional geometry of the vocal fold model (Panel A) and the three-dimensional vocal fold model with fibers (long dashed lines) embedded in the cover layer (Panel B) and the body layer (Panel C). In Panel B, two fiber bundles each were used at the superior and inferior locations, and three bundles were used at the medial location. Seven fiber bundles were used in Figure 2, Panel C.

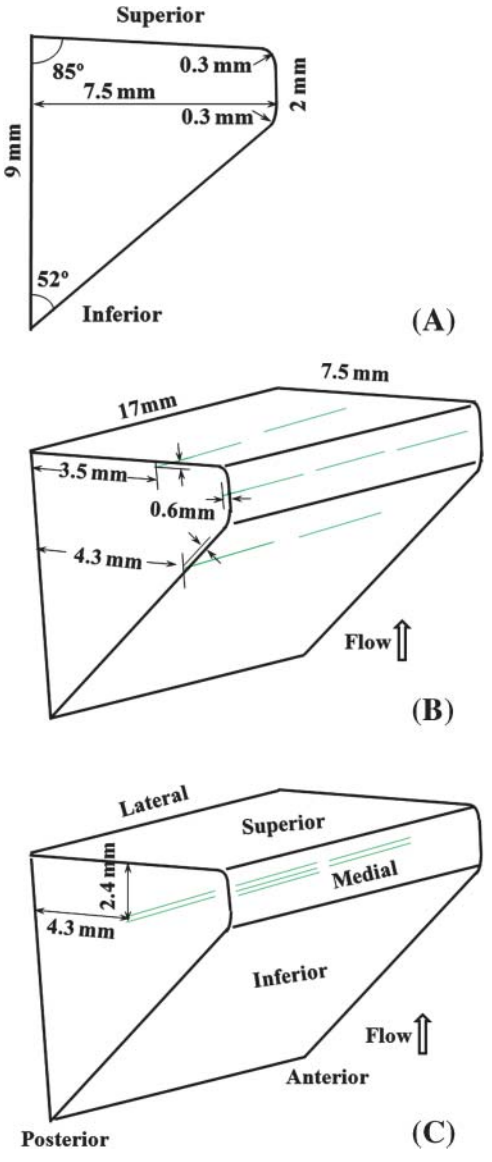

variables. In comparison, embedding short fibers in this study had a smaller effect.

Figure 4 shows superior-view images of the seven vocal fold models at onset during one oscillation cycle. The extracted glottal area waveforms are shown in Figure 5. The baseline model M1 did not produce complete glottal closure, with a minimum glottal area of approximately 10 mm^2. Compared with the baseline model, embedding fibers in the body layer did not reduce the minimum glottal area but noticeably reduced the maximum glottal opening area and thus did not improve the closure pattern. Embedding fibers in the cover layer, however, allowed the glottis to reach complete closure (as indicated by the minimum glottal area of zero), although only briefly, and also led to an increased maximum glottal opening area. The most significant improvement in the glottal closure pattern was achieved by the addition of a stiffer outer layer in M4–M6. Complete glottal closure was achieved in all three models with a stiffer outer layer (M4, M5, and M6), with or without fibers. The longest closure time was achieved in M6, which had both the epithelium layer and fibers in the cover layer, with a closed quotient of 0.29, and decreased to 0.14 and 0.13 in M5 and M4, respectively.

The addition of the epithelium layer and fibers also led to changes in the transition pattern of the medial surface profile (from convergent, straight, and back to divergent) during one oscillation cycle. Figure 5 also shows the instants (solid symbols) at which the medial surface changed between divergent and convergent profiles. These transition instants were determined by manually stepping through consecutive frames and locating the frame in which a lower margin of the vocal folds first became either visible or hidden below the upper margin of the vocal folds. (Note that, because of prephonatory vocal fold deformation due to the applied subglottal pressure, the portion of the vocal fold surface between the observed upper and lower margins, or the actual medial surface, spanned a much larger vertical area than the predefined medial surface indicated in Figure 2.) All seven models had a convergent medial surface shape during glottal opening and changed to a divergent medial surface around the moments of maximum opening. However, the transition from a divergent to a convergent medial surface shape occurred at a much later time during the closing phase for M3–M6 than M1 and M2. As the intraglottal pressure is generally lower or even negative for a divergent medial surface than for a convergent medial surface profile (Scherer et al., 2001), such late transition from a divergent to convergent medial surface profile may facilitate complete glottal closure.

Table 1. Structural composition of the seven vocal fold models used in this study.

Variable	M1	M2	M3	M4	M5	M6	M7
Epithelium	No	No	No	Yes	Yes	Yes	No
Fiber location	No fibers	Body	Cover	No fibers	Body	Cover	No fibers
Length (mm)	17	17	17	17	17	17	12

Figure 3. Panel A: The phonation threshold pressure P_{th} (○) and onset frequency F_0 (■) in the seven vocal fold models. Panel B: Onset flow rate (◊) and outside sound pressure amplitude (▲) at onset in the seven vocal fold models.

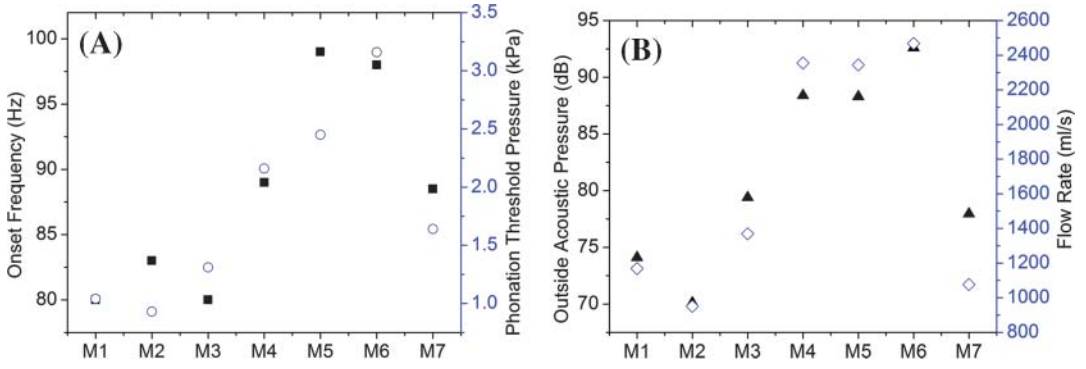

For models with complete glottal closure, the vocal folds vibrated roughly in-phase along the AP direction, whereas notable out-of-phase motion along the AP direction was observed in models without complete closure. The phase difference in the medial–lateral motion along the AP length for each model is illustrated in Figure 6, which compares the time history of the superior-view images of two medial–lateral slices taken from the middle and the anterior quarter along the AP direction of the seven vocal fold models. For ease of comparison, the time-history plot for the anterior-quarter

Figure 4. Superior-view images of the seven vocal fold models at equal intervals during one oscillation cycle.

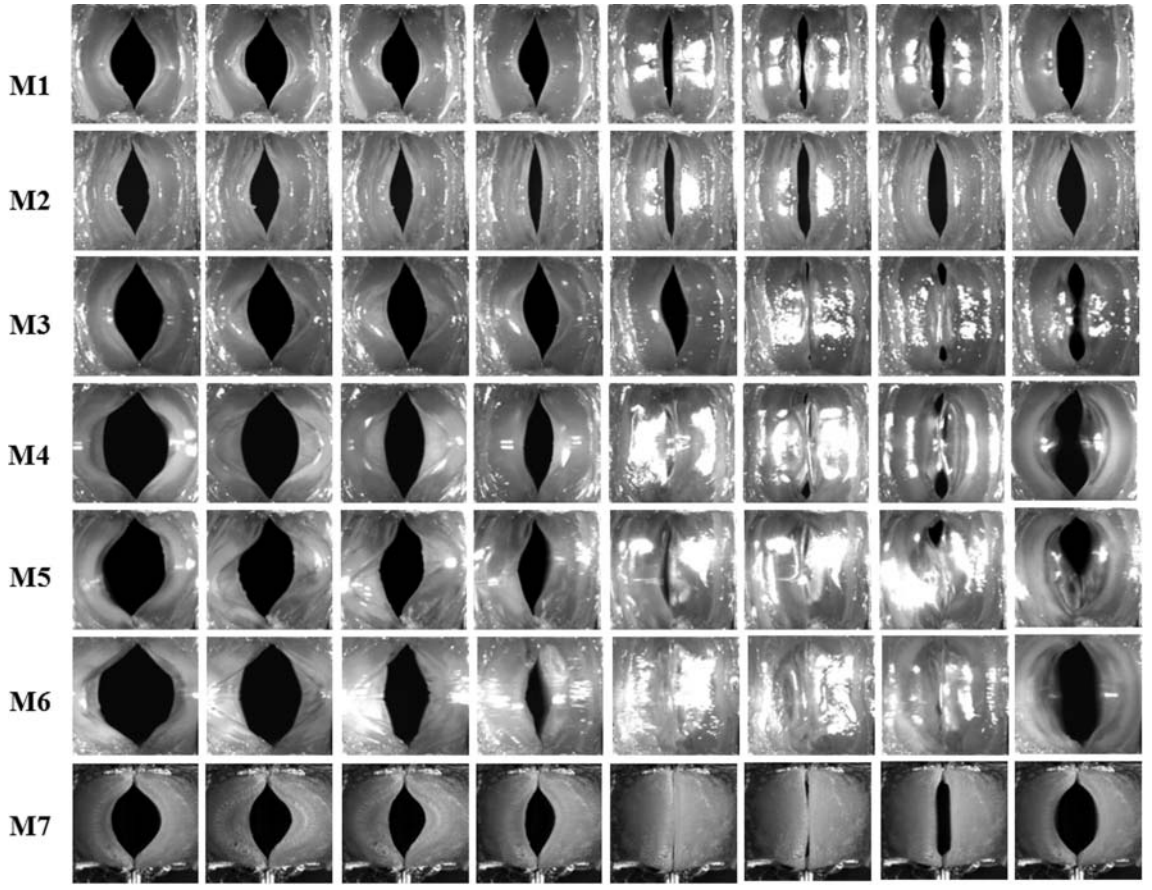

Figure 5. Glottal area waveforms extracted from the superior-view images in Figure 4. The first solid symbol on each curve indicates the instant when the medial surface shape changed from convergent to divergent during glottal opening, and the second solid symbol indicates the instant when the medial surface shape changed from divergent to convergent during the closing phase.

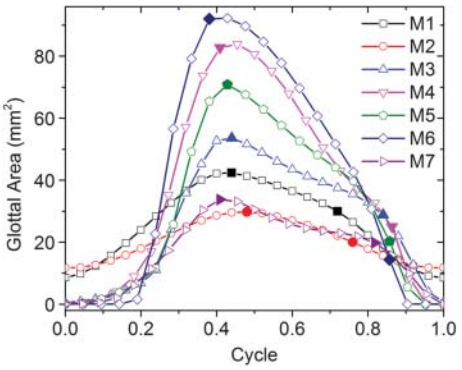

slice was flipped so that the medial edges of the two slices faced each other in each subplot. For models with complete glottal closure (M3–M6), the vocal fold medial surface generally vibrated in a more in-phase pattern along the AP direction so that the entire vocal fold edge along the AP direction moved in and out toward the glottal midline together. In contrast, for models with incomplete glottal closure (M1 and M2), the vocal fold edge exhibited a noticeable out-of-phase medial–lateral motion along the AP direction, particularly during instants of glottal closure (indicated by the arrows in the figure). Specifically, the middle part moved toward the glottal midline when the anterior portion was already moving away from the glottal midline, thus preventing complete glottal closure.

The same experiments were repeated four times using different sets of models with either dry powder or wet lubricant agents spread on the surfaces of the models. No qualitative difference in the glottal closure pattern was observed despite the fact that these models were made at different times and of different surface conditions.

The fact that complete glottal closure was accompanied by a more in-phase motion along the AP direction suggests that suppression of the out-of-phase motion may facilitate complete glottal closure. To test this hypothesis, we performed an additional experiment using M7, which was an isotropic vocal fold model identical to M1 except for a reduced length of 12 mm. Reducing vocal fold length along the AP direction shifts the AP out-of-phase motion to high-order eigenmodes and thus may suppress the occurrence of the AP out-of-phase motion during vibration (Zhang, 2011). This was confirmed in Figure 6, which shows that the medial surface moved almost in-phase along the AP direction in M7. Figures 4 and 5 also show that the glottal closure in M7 was much improved from that of M1, despite the fact that both models were isotropic.

Figure 7 shows the spectra of the outside sound pressure at onset for the seven vocal fold models. In general, improvement in the glottal closure pattern led to more excitation of high-order harmonics in the outside sound spectra, comparing M3–M7 with M1–M2, and produced a brighter sound quality in M3–M7. On the other hand, models with a large vibration amplitude also led to increased noise production, presumably due to the large flow rate.

Discussion and Conclusion

Although one-layer isotropic vocal fold models often vibrated with incomplete glottal closure, this study showed that adding a stiffer outer layer or embedding fibers along

Figure 6. Comparison between the time history of the superior-view images of two medial–lateral slices taken from the middle and the anterior quarter along the anterior–posterior direction in the seven vocal fold models. The vertical position of the arrows indicates the instant of maximum medial excursion of the corresponding vocal fold slice, with the difference in the vertical position of the two arrows in each subplot indicating the degree of phase difference between the anterior and middle slices. The phase difference in the medial–lateral motion between the middle and the anterior slices was reduced in models M3–M7 compared with models M1–M2.

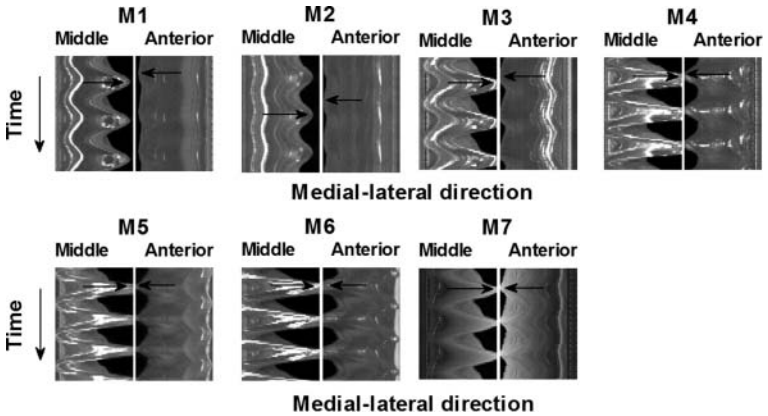

Figure 7. Spectra of the outside sound pressure slightly above onset in all seven vocal fold models.

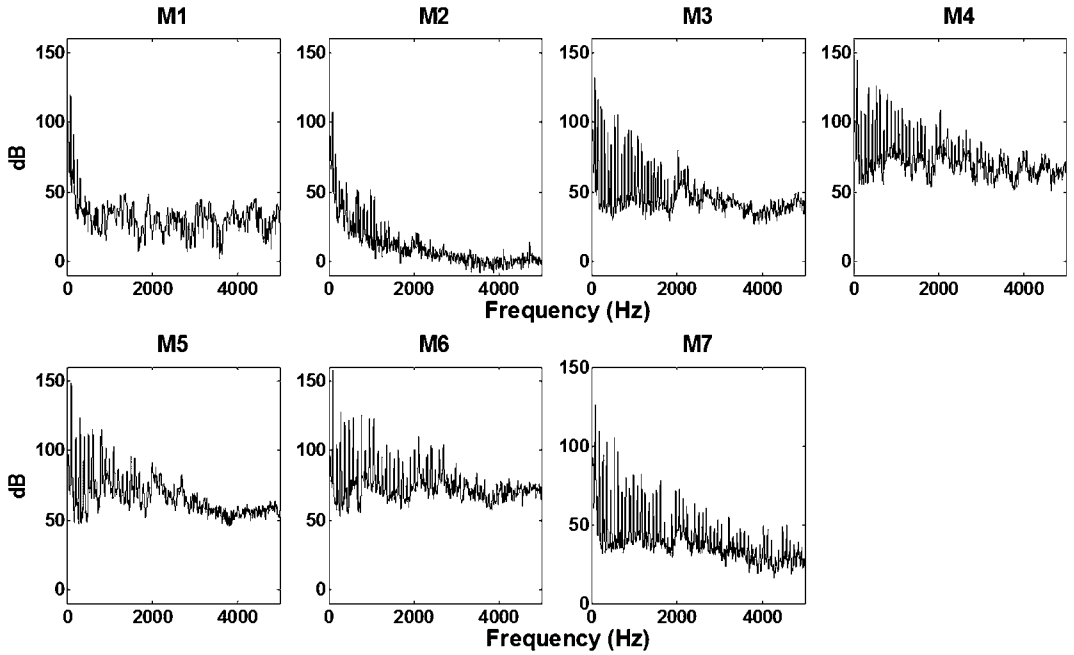

the AP direction in the cover layer was able to produce complete glottal closure with a closed quotient as high as 0.29. Although use of the embedded fibers in the cover layer was less effective than use of an epithelium layer in this study, which was probably due to the small number of fibers used and the short fiber length, the improvement in the glottal closure pattern was achieved without noticeable increase in the phonation threshold pressure. In contrast, the presence of the epithelium layer was the most effective but also led to a significant increase in the phonation threshold pressure in M4–M6. The stiffer outer epithelium layer used in this study had a thickness of approximately 130±20 μm, which was approximately twice the reported thickness of the epithelium in human vocal fold (Hirano & Kakita, 1985). Thus, it is possible that the influence of the epithelium layer on the glottal closure pattern and the phonation threshold pressure in humans may not be as large as observed in this study.

Similar features of embedded fibers and a stiffer epithelium layer were implemented earlier in Murray and Thomson (2012). In that study, although the presence of an epithelium layer and a fiber bundle (with and without pretension) led to a convergent–divergent motion of the vocal fold motion, the model did not appear to vibrate with complete glottal closure or a closed quotient as large as in the present study. Many factors may have contributed to this difference in the glottal closure pattern. The epithelium layer and the fiber bundle in Murray and Thomson were made from a different, softer material than that used in the present study. In addition, the fiber bundle in Murray and Thomson was located further away from the vocal fold surface compared with that in the present study, which, as indicated in our results in M2, did not provide much improvement in achieving complete glottal closure. Last, it is important to note that the model used in Murray and Thomson was a multilayer model, which does not present a fair comparison to the one-layer model (other than the fibers and epithelium layer) of the present study.

Because complete glottal closure in M4–M6 was accompanied by a significant increase in phonation threshold pressure, one may argue that the observed complete glottal closure in M4–M6 was due to the extremely high phonation threshold pressure in these models. However, in our previous experiments, as well as in this study, increasing the subglottal pressure further beyond onset in the isotropic one-layer model led to an almost proportionate increase in both the mean glottal area and the vibration amplitude, and thus still incomplete glottal closure. Figure 8 shows the equal-interval superior-view images of an M1 model (fabricated at a later time) during one oscillation cycle at five different subglottal pressures. The first condition corresponded to a subglottal pressure slightly above onset at 1.06 kPa, whereas the last condition was for a subglottal pressure of 2.17 kPa, at which point the model started to fracture due to collision. Compared with that at onset, the minimum glottal opening decreased only slightly with increasing subglottal pressure. The main effect of increasing subglottal pressure was to increase the vibration amplitude of the vocal fold in the middle portion along the AP direction. High subglottal pressures also led to a left–right asymmetric vibration pattern (Figure 8d–8e). Further increase in the subglottal pressure beyond 2.17 kPa led to model damage due to extremely large vibration amplitude, thinning, and strong collision in the

Figure 8. Superior-view images of the isotropic one-layer model M1 at equal intervals during one oscillation cycle. The mean subglottal pressure was (Row A) 1.06 kPa (slightly above onset); (Row B) 1.25 kPa; (Row C) 1.46 kPa; (Row D) 1.92 kPa; and (Row E) 2.17 kPa.

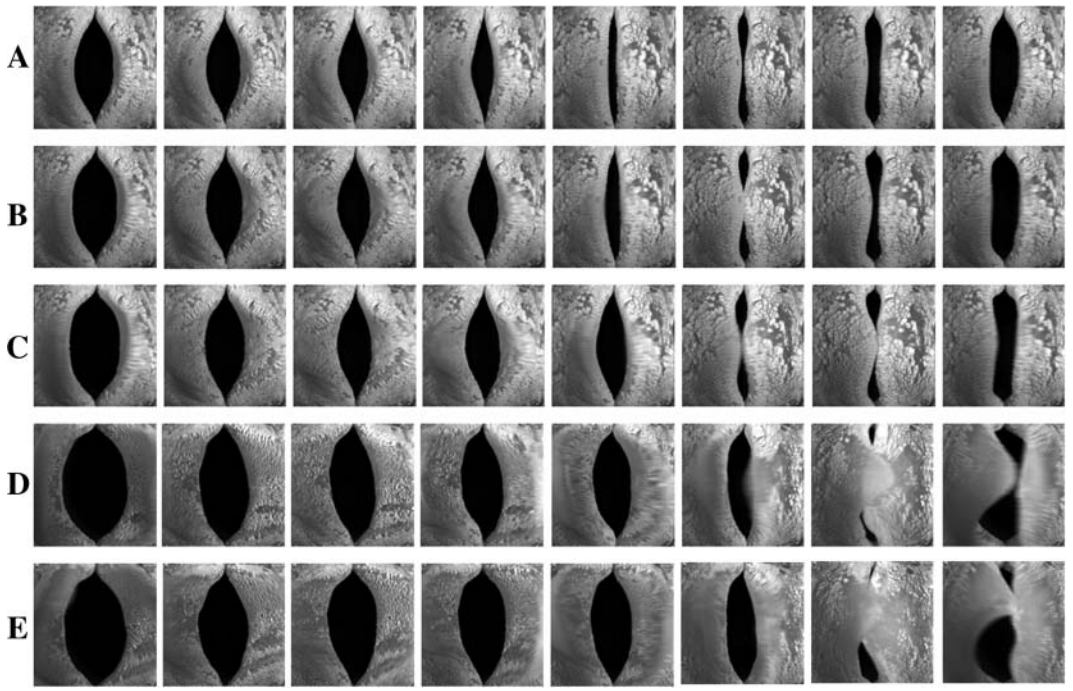

middle portion of the vocal fold model. The incomplete glottal closure in M1 at high subglottal pressures was in contrast to M4–M6, which vibrated with complete glottal closure at comparable values of subglottal pressure. Thus, the observed improvement in the glottal closure pattern in M4–M6 cannot be explained by the increase in phonation threshold pressure alone. The comparison between M1 and M4 also indicated that one function of the stiffer epithelium layer is to protect the soft inner layers of the vocal folds from extreme deformation and damage, as suggested in Murray and Thomson (2012).

Previous studies have achieved improved glottal closure by stiffening the vocal fold body to restrain the mean deformation (Zhang, 2011; Zhang et al., 2006a), that is, reduce the mean glottal opening for a given constant subglottal pressure. In this study, both the stiffer outer layer and the embedded fibers provided similar restraining effect. However, this restraining effect applied equally to both the mean glottal opening and the vibration amplitude, as shown in Figure 9. Figure 9a shows the mean glottal opening area and the glottal vibration amplitude (estimated as half of the peak-to-peak value of the glottal area waveform in Figure 5) for all seven vocal fold models. Figure 9b shows the mean glottal area normalized by the phonation threshold pressure (the time-averaged subglottal pressure at onset) and the glottal vibration amplitude normalized by the subglottal acoustic pressure (the fluctuating component of the subglottal pressure). Although the glottal vibration amplitude increased at a higher rate than the mean glottal area with the addition of a stiffer outer layer or embedded fibers in the cover layer, Figure 9b shows that, although the presence of an epithelium layer and the fibers reduced the mean glottal opening for a given mean subglottal pressure, it also reduced the vocal fold vibration amplitude for a given amplitude of the subglottal acoustic pressure. This suggests that restraining the prephonatory vocal fold deformation alone is not enough to achieve complete glottal closure.

Because phonation generally occurs as two or more vocal fold eigenmodes (i.e., resonances of the vocal fold structure) are synchronized (Zhang, 2010; Zhang, Neubauer, & Berry, 2007), it is possible that both structural modifications significantly changed the eigenmodes of the vocal fold in a way that alters the fluid-structure interaction and energy transfer from airflow to the vocal folds. For example, the results from M7 seem to indicate that suppression of the AP out-of-phase motion, particularly during the closing phase, facilitates complete glottal closure. The suppression of the AP out-of-phase motion and the occurrence of a more in-phase motion would also enhance flow modulation and may increase sound production efficiency. Further investigation of the eigenmode synchronization pattern in the presence of the out-of-phase eigenmodes or in vocal folds of different structural features is required to elucidate the mechanisms underlying the observation of this study. Such an improved understanding of the mechanisms underlying complete glottal closure would provide a theoretical foundation based on which better diagnosis and treatment of various voice disorders can be achieved.

Figure 9. Panel A: The mean glottal opening area (■) and the glottal area amplitude (○; estimated as the half of the peak-to-peak value of the glottal area waveform). Panel B: The mean glottal opening area normalized by the phonation threshold pressure (◊) and the glottal vibration amplitude normalized by the subglottal acoustic pressure (▲).

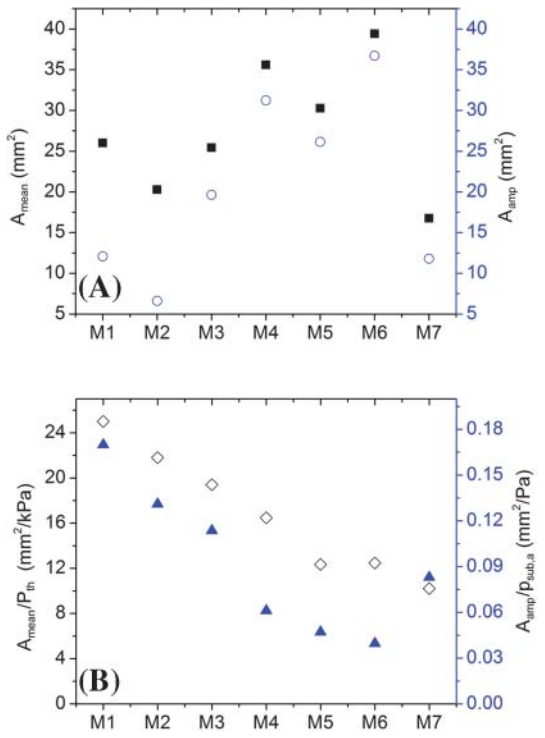

Although no vocal tract was used in the experiments reported in this study, no obvious changes in the glottal closure pattern (e.g., the minimum and maximum glottal area) were observed in our preliminary experiments when a uniform vocal tract model was attached to the vocal fold model. The presence of the vocal tract did, however, lead to increased harmonic production in the output sound spectra, which occurred for all seven vocal fold models and was presumably due to the acoustic resonances of the vocal tract tube. Nevertheless, a systematic investigation using different vocal tract shapes is justified, and the acoustic effects of the vocal tract and possible source-tract interaction will be addressed in a separate study. Last, we note that the results reported in this study were based on one particular physical model and one specific geometry. Although we anticipate that the general observations of this study will remain qualitatively the same, future studies using different physical models and vocal fold geometry are required to confirm and generalize the findings of this study to human phonation.

Acknowledgments

This study was supported by National Institute on Deafness and Other Communication Disorders Grants R01 DC011299 and R01DC009229, awarded to the second author. Portions of this work were presented at the 165th meeting of the Acoustical Society of America, Montreal, Canada, June 2013.

References

Chan, R., Titze, I. R., & Titze, M. (1997). Further studies of phonation threshold pressure in a physical model of the vocal fold mucosa. *The Journal of the Acoustical Society of America, 101,* 3722–3727.

Chhetri, D. K., Zhang, Z., & Neubauer, J. (2011). Measurement of Young's modulus of vocal fold by indentation. *Journal of Voice, 25,* 1–7.

Gunter, H. E. (2003). *Mechanical stresses in vocal fold tissue during voice production* (Doctoral dissertation). Harvard University, Cambridge, MA. Retrieved from www.biorobotics.harvard.edu/pubs/hgthesis.pdf

Hirano, M., & Kakita, Y. (1985). Cover-body theory of vocal fold vibration. In R. G. Daniloff (Ed.), *Speech science: Recent advances* (pp. 1–46). San Diego, CA: College Hill Press.

Kniesburges, D., Thomson, S., Barney, A., Triep, M., Sidlof, P., & Horacek, J. (2011). In vitro experimental investigation of voice production. *Current Bioinformatics, 6,* 305–322.

Krebs, F., Artana, G., & Sciamarella, D. (2010, April). *Constriction modes and acoustic output in an in-vitro self-oscillating vocal-fold model*. Paper presented at the 10ème Congrès Français d'Acoustique, Lyon, France. Retrieved from http://en.youscribe.com/catalogue/reports-and-theses/knowledge/natural-science/constriction-modes-and-acoustic-output-in-an-in-vitro-1488485

Mendelsohn, A., & Zhang, Z. (2011). Phonation threshold pressure and onset frequency in a two-layer physical model of the vocal folds. *The Journal of the Acoustical Society of America, 130,* 2961–2968.

Murray, P. R., & Thomson, S. L. (2012). Vibratory responses of synthetic, self-oscillating vocal fold models. *The Journal of the Acoustical Society of America, 132,* 3428–3438.

Ruty, N., Pelorson, X., Van Hirtum, A., Lopez-Arteaga, I., & Hirschberg, A. (2007). An in vitro setup to test the relevance and the accuracy of low-order vocal folds models. *The Journal of the Acoustical Society of America, 121,* 479–490.

Scherer, R. C., Shinwari, D., De Witt, K. J., Zhang, C., Kucinschi, B. R., & Afjeh, A. A. (2001). Intraglottal pressure profiles for a symmetric and oblique glottis with a divergence angle of 10 degrees. *The Journal of the Acoustical Society of America, 109,* 1616–1630.

Shaw, S. M., Thomson, S. L., Dromey, C., & Smith, S. (2012). Frequency response of synthetic vocal fold models with linear and nonlinear material properties. *Journal of Speech, Language, and Hearing Research, 55,* 1395–1406.

Stevens, K. N. (1998). *Acoustic phonetics*. Cambridge, MA: MIT Press.

Thomson, S. L., Mongeau, L., & Frankel, S. H. (2005). Aerodynamic transfer of energy to the vocal folds. *The Journal of the Acoustical Society of America, 118,* 1689–1700.

Titze, I. R., Schmidt, S. S., & Titze, M. R. (1995). Phonation threshold pressure in a physical model of the vocal fold mucosa. *The Journal of the Acoustical Society of America, 97,* 3080–3084.

van den Berg, J. W., & Tan, T. S. (1959). Results of experiments with human larynxes. *Practica Oto-Rhino-Laryngologica, 21,* 425–450.

Zhang, Z. (2010). Dependence of phonation threshold pressure and frequency on vocal fold geometry and biomechanics. *The Journal of the Acoustical Society of America, 127,* 2554–2562.

Zhang, Z. (2011). Restraining mechanisms in regulating glottal closure during phonation. *The Journal of the Acoustical Society of America, 130,* 4010–4019.

Zhang, Z., Neubauer, J., & Berry, D. A. (2006a). Aerodynamically and acoustically driven modes of vibration in a physical model of the vocal folds. *The Journal of the Acoustical Society of America, 120,* 2841–2849.

Zhang, Z., Neubauer, J., & Berry, D. A. (2006b). The influence of subglottal acoustics on laboratory models of phonation. *The Journal of the Acoustical Society of America, 120,* 1558–1569.

Zhang, Z., Neubauer, J., & Berry, D. A. (2007). Physical mechanisms of phonation onset: A linear stability analysis of an aeroelastic continuum model of phonation. *The Journal of the Acoustical Society of America, 122,* 2279–2295.

Zhang, Z., Neubauer, J., & Berry, D. A. (2009). Influence of vocal fold stiffness and acoustical loading on flow-induced vibration of a single-layer vocal fold model. *Journal of Sound and Vibration, 322,* 299–313.